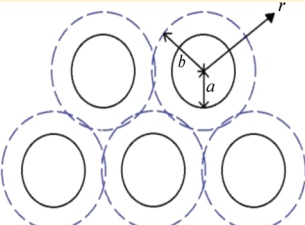# Electrokinetic Flow and Electric Current in a Fibrous Porous Medium

Yi Y. Wu and Huan J. Keh*

Department of Chemical Engineering, National Taiwan University, Taipei 10617, Taiwan, Republic of China

ABSTRACT: An analytical study is presented for the steady electrokinetic flow of electrolyte solutions in the fibrous medium constructed by an ordered array of identical, parallel, charged, circular cylinders. The electric field and/or pressure gradient are applied uniformly in the direction along the axes of the cylinders. The dielectric cylinders may have either a constant surface potential or a constant surface charge density of an arbitrary value. The electric double layer surrounding each cylinder may have an arbitrary thickness relative to the radius of the cylinder. A unit cell model, which allows for the overlap of the double layers of adjacent cylinders, is employed to account for the effect of fiber interactions. The electrostatic potential distribution in the fluid phase is determined by solving the Poisson−Boltzmann equation, and the fluid velocity profile is obtained as the analytical solution of a modified Navier−Stokes equation. Explicit formulas for the flow rate, electroosmotic velocity, electric current, effective electric conductivity, and streaming potential are derived as functions of the porosity of the fiber matrix and other characteristics of the system. The effect of interactions among the cylinders on the fluid velocity and effective conductivity is interesting and can be significant under appropriate conditions.

$$u = \frac{P}{4\eta}[2b^2 \ln \frac{r}{a} + a^2 - r^2]$$
$$- \frac{\varepsilon E}{\eta}[\zeta - \psi(r)]$$
$$<u> = L_{11}P + L_{12}E$$
$$<i> = L_{21}P + L_{22}E$$

1. INTRODUCTION

Electrokinetics is the general term associated with the relative motion of two adjacent charged phases. In the study of phenomena occurring at charged solid−liquid interfaces, electrokinetic methods, such as electrophoresis, electroosmosis, sedimentation potential, and streaming potential, have proved to be useful tools. The basic relationships involved in electrokinetic phenomena were derived mainly for the migration of a single charged colloidal particle[1−10] or for the ionic fluid motion and electric current flow in a single microchannel with surface charges.[11−17]

In many applications of the electrokinetic flow of ionic solutions in practice, porous media are usually encountered, and the effect of interactions among the solid entities will be important. To avoid the difficulty of the complex geometry appearing in swarms of solid entities, a unit cell model has usually been used to predict the effect of entity interactions on various transport properties, such as the mean electroosmotic velocity,[18−25] effective electric conductivity,[22−28] and average diffusioosmotic velocity,[29−31] in porous systems of ordered solid entities. This model involves the concept that a swarm of small entities can be divided into a number of identical cells and each entity occupies a cell at its center. The boundary-value problem for multiple entities is thus reduced to the one for a single entity and its bounding envelope. Although different shapes of the cell can be employed, the assumption of a spherical[18,22−26,30−35] or cylindrical[19−21,27,29,36] shape for the fictitious envelope of fluid surrounding each spherical or cylindrical entity is of great convenience in mathematical manipulation.

Through the use of the unit cell model, the electroosmosis and electric conduction of electrolyte solutions in a bed of dielectric spheres with a small surface potential and an arbitrary

thickness of the electric double layers were investigated with the assumption that the system is only slightly distorted from equilibrium, and analytical formulas for the mean electroosmotic velocity and effective electric conductivity were obtained as functions of the electrokinetic radius and volume fraction of the particles correct to the second order of the surface potential.[23] These formulas are in better agreement with the available experimental data for suspensions of charged spheres with various particle volume fractions[37,38] than earlier predictions.[26,39,40] Recently, using the unit cell model, we also obtained the corresponding formulas for electrolyte solutions in an ordered array of parallel circular cylinders under a transversely imposed electric field.[41]

In this article, we analyze the electrokinetic flow of electrolyte solutions in a homogeneous fibrous system constructed by an array of parallel circular cylinders generated by an axially applied electric field and/or pressure gradient. The unit cell model is still used in the analysis. The surface charge density or potential of the cylinders is assumed to be uniform, but no assumption is made as to its magnitude or the thickness of the electric double layers relative to the radius of the cylinders. Explicit expressions for the fluid velocity profile and effective electric conductivity in a cell are obtained in eqs 14 and 23.

2. ELECTROSTATIC POTENTIAL DISTRIBUTION

We consider the electrokinetic flow of an electrolyte solution in the fibrous medium constructed by a uniform array of parallel, identical, circular cylinders. The discrete nature of the surface

charges, which are uniformly distributed on each dielectric cylinder, is neglected. Both a constant electric field and a uniform pressure gradient are applied along the axial (z) direction of the fiber cylinders, whereas the electrolyte concentration is independent of the axial position. As shown in Figure 1, we employ a unit cell model in which each cylinder
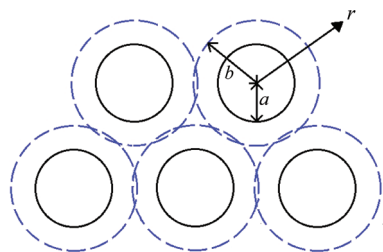
Figure 1. Geometrical sketch of the unit cell model for a uniform array of parallel, identical, circular cylinders.

of radius a is surrounded by a coaxial circular cylindrical shell of the fluid solution having an outer radius of b such that the fluid/cell volume ratio is equal to the porosity $1-\varphi$ of the fiber matrix; viz., $\varphi = (a/b)^2$. The cell as a whole is electrically neutral.

2.1. General Analysis. Since the applied electric field and pressure gradient are along the axial direction and there is no concentration gradient of the electrolyte in this direction, the space charge density of the fluid solution in a unit cell is a function of the radial position only and can be determined from the equilibrium electrostatic potential. If $\rho_e(r)$ represents the space charge density of the electrolyte solution at a position with distance r from the axis of the cylinder in a cell and $\psi(r)$ denotes the equilibrium potential at this position relative to that in the bulk (electrically neutral) solution, then Poisson's equation gives

$$\frac{1}{r}\frac{d}{dr}\left(r\frac{d\psi}{dr}\right) = -\frac{\rho_e}{\varepsilon} \tag{1}$$

where ε is the dielectric permittivity of the electrolyte solution, which is taken to be constant.

The space charge density can also be related to the electrostatic potential by the Boltzmann equation,

$$\rho_e = \sum_m z_m e n_m^\infty \exp\left(-\frac{z_m e\psi}{kT}\right) \tag{2}$$

where n_m^∞ is the concentration of the ionic species m in the bulk solution phase in equilibrium with the fluid inside the cell, z_m is the valence of the ionic species m, e is the charge of a proton, k is the Boltzmann constant, and T is the absolute temperature. Substitution of eq 2 into eq 1 leads to the well-known Poisson–Boltzmann equation,

$$\frac{1}{r}\frac{d}{dr}\left(r\frac{d\psi}{dr}\right) = -\frac{e}{\varepsilon}\sum_m z_m n_m^\infty \exp\left(-\frac{z_m e\psi}{kT}\right) \tag{3}$$

For the case of constant surface potential, the boundary conditions for ψ are

$$r = a, \quad \psi = \zeta \tag{4}$$

$$r = b, \quad \frac{d\psi}{dr} = 0 \tag{5}$$

where the constant ζ is the zeta potential of the cylinder in the electrolyte solution. Equation 5 for the cell model allows for the overlap of the electric double layers of adjacent cylinders in the fibrous array. If the constant surface charge density σ, instead of the surface potential ζ, is known on the cylinder, the boundary condition specified by eq 4 should be replaced by the Gauss condition,

$$r = a, \quad \frac{d\psi}{dr} = -\frac{\sigma}{\varepsilon} \tag{6}$$

There is no simple analytical solution of eq 3 available for the case of cylindrical symmetry. Following the classic approach developed by Philip and Wooding[42] for a circular cylindrical particle in an unbounded fluid (with $b/a \to \infty$), Keh and Hsu[43] recently obtained a good approximate solution for $\psi(r)$ satisfying eq 3 for fluid solutions of symmetrically charged binary electrolytes subject to the boundary conditions given in eqs 5 and 4 or 6 in explicit but complex forms for arbitrary values of a/b and ζ or σ. This approximate solution will be used for the calculations in the following sections.

2.2. Case of Low Electric Potential. When the surface potential ζ is small, the Poisson–Boltzmann equation can be linearized (known as the Debye–Huckel approximation), and eq 3 becomes

$$\frac{1}{r}\frac{d}{dr}\left(r\frac{d\psi}{dr}\right) = \kappa^2\psi \tag{7}$$

where $\kappa = (\sum_m n_m^\infty z_m^2 e^2/\varepsilon kT)^{1/2}$ is the Debye screening parameter. The solution to eqs 7, 4, and 5 is

$$\psi = \zeta\frac{G_0(r)}{G_0(a)} \tag{8}$$

where

$$G_n(r) = I_1(\kappa b)\,K_n(\kappa r) + (-1)^n K_1(\kappa b)\,I_n(\kappa r) \tag{9}$$

I_n and K_n are the modified Bessel functions of the first and second kinds, respectively, of order n.

The solution for ψ expressed by eq 8 also holds for the condition 6 of constant surface charge density, with the relation between ζ and σ for arbitrary values of κa and κb (κ is related to the electrolyte concentration) as

$$\zeta = \frac{\sigma}{\varepsilon\kappa}\frac{G_0(a)}{G_1(a)} \tag{10}$$

Due to the linearization of the Poisson–Boltzmann equation, the normalized potential distribution ψ/ζ given by eq 8 is independent of the dimensionless parameters $z_m e\zeta/kT$. Note that the approximate solution for $\psi(r)$ satisfying eqs 3, 5, and 4 or 6 available in the literature[43] is the same as eqs 8–10 for the case of small surface potential ($|z_m\zeta|e/kT \leq 1$).

3. FLUID VELOCITY DISTRIBUTION

We now consider the steady flow of an electrolyte solution through a cylindrical unit cell under the influence of a constant electric field E and a uniform dynamic pressure gradient P, both applied axially.

3.1. General Analysis. The momentum balance on the Newtonian fluid (the modified Navier−Stokes equation) in the z direction gives

$$\frac{\eta}{r}\frac{d}{dr}\left(r\frac{du}{dr}\right) = -P - \rho_e E \qquad (11)$$

where $u(r)$ is the fluid velocity in the direction of E or opposite direction of P, which satisfies the equation of continuity for an incompressible fluid, η is the viscosity of the fluid, and ρ_e is given by eq 2. The boundary conditions for u are

$$r = a, \quad u = 0 \qquad (12)$$

$$r = b, \quad \frac{du}{dr} = 0. \qquad (13)$$

Solving for the fluid velocity distribution subject to eqs 11−13, we obtain

$$u = \frac{P}{4\eta}\left[2b^2 \ln\frac{r}{a} + a^2 - r^2\right] - \frac{\varepsilon E}{\eta}[\zeta - \psi(r)] \qquad (14)$$

where the electrostatic potential distribution $\psi(r)$ has been discussed in the previous section.

The average (superficial) fluid velocity over a cross section of the unit cell can be expressed as

$$\langle u \rangle = L_{11}P + L_{12}E \qquad (15)$$

where L_{11} and L_{12} are the so-called Onsager transport coefficients and the definition of the angle brackets is

$$\langle u \rangle = \frac{2}{b^2}\int_a^b u(r)r\,dr \qquad (16)$$

Substituting eq 14 into eq 16, performing the integration, and comparing the result with eq 15, we obtain

$$L_{11} = \frac{a^2}{8\eta}[4 - \varphi - 3\varphi^{-1} - 2\varphi^{-1}\ln\varphi] \qquad (17)$$

$$L_{12} = -\frac{\varepsilon}{\eta}\left[(1 - \varphi)\zeta - \frac{2\varphi}{a^2}\int_a^b \psi(r)r\,dr\right] \qquad (18)$$

with the relation $b = a\varphi^{-1/2}$.

The electroosmotic velocity profile $u^{(e)}(r)$ in a unit cell is given by eq 14 with $P = 0$. The average electroosmotic velocity over a cross section of the cell, $\langle u^{(e)} \rangle = L_{12}E$, needs to be calculated using eq 18. Also, the electroosmotic counter pressure (gradient) can be obtained by $P = -EL_{12}/L_{11}$ from eq 15 under the condition of no net fluid flow (viz., $\langle u \rangle = 0$). Substitution of this counter pressure into eq 14 results in the fluid velocity profile for the case of vanishing flow rate. Note that $u^{(e)}(b)$, the electroosmotic velocity at the outer boundary of a unit cell, can also be viewed as the electrophoretic velocity (in the opposite direction) of the charged cylinder in the cell caused by the imposed electric field. For the limiting case of $\varphi = 0$ ($b \to \infty$), this axial electroosmotic or electrophoretic velocity reduces to the Helmholtz−Smoluchowski formula $[u^{(e)}(b\to\infty) = -\varepsilon\zeta E/\eta]$ no matter what the values of κa and $e\zeta/kT$ are.

3.2. Case of Low Electric Potential. When the surface potential ζ of the cylinder is small, the potential distribution $\psi(r)$ in the unit cell is given by eq 8 and then eq 18 becomes

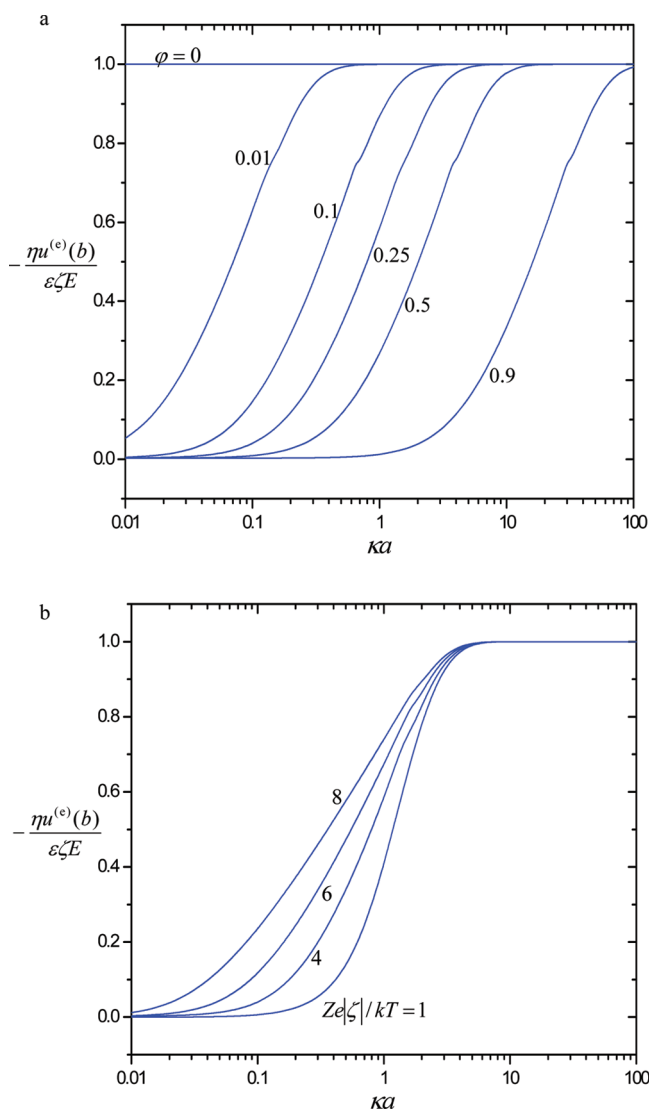$$L_{12} = -\frac{\varepsilon}{\eta}\zeta\left[1 - \frac{G_2(a)}{G_0(a)}\varphi\right] \qquad (19)$$

3.3. Results and Discussion. To present the results for the electrokinetic flow, we consider the fluid solution of a symmetrically charged electrolyte of valence Z ($z_+ = -z_- = Z$, where subscripts $+$ and $-$ refer to the cation and anion, respectively). The normalized electroosmotic velocity distribution $-\eta u^{(e)}(r)/\varepsilon\zeta E$ of the electrolyte solution around an isolated circular cylinder ($\varphi=0$) in the axial direction given by eq 14 with $P = 0$ is plotted versus the dimensionless coordinate r/a in Figure 2 for different values of the electrokinetic radius κa and dimensionless zeta potential $Z e\zeta/kT$. The approximate solution for the potential distribution $\psi(r)$ available in the literature,[42,43] which is the same as eq 8 taking $b/a \to \infty$ for the case of $Ze|\zeta|/kT \leq 1$, is used for the calculations. As expected, for specified finite values of the parameters κa and $Ze\zeta/kT$, this normalized fluid velocity increases monotonically with r/a from
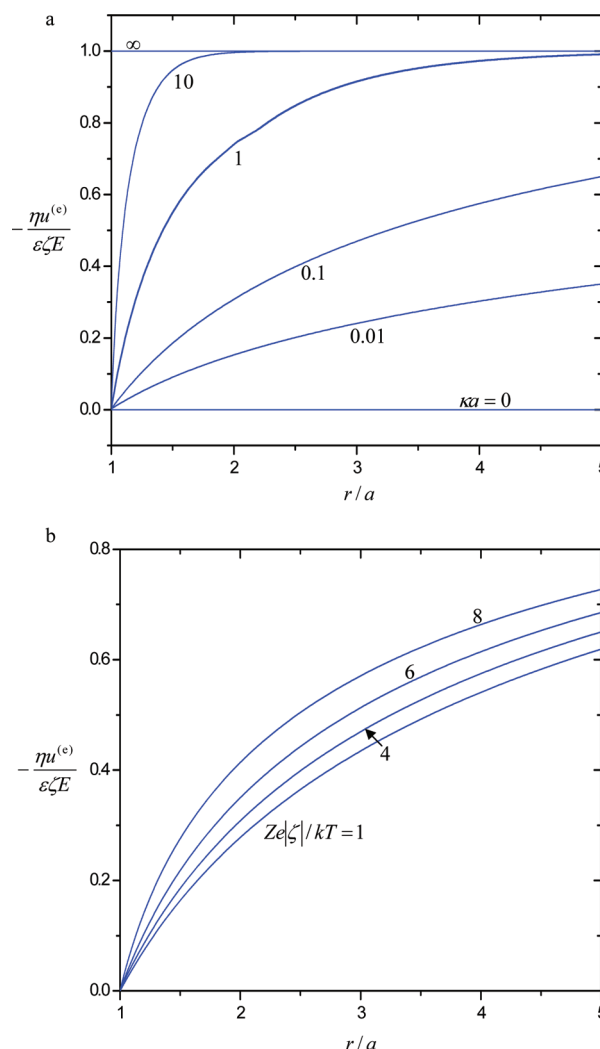
Figure 2. Plots of the normalized electroosmotic velocity $-\eta u^{(e)}(r)/\varepsilon\zeta E$ of a symmetric electrolyte solution around an isolated circular cylinder ($\varphi = 0$) in the axial direction versus the dimensionless coordinate r/a: (a) $Ze|\zeta|/kT = 4$ and (b) $\kappa a = 0.1$.

zero at the no-slip surface (shear plane) of the cylinder ($r/a = 1$) to unity far away from the cylinder ($r/a \rightarrow \infty$). For fixed values of r/a and $Ze\zeta/kT$, $-\eta u^{(e)}(r)/\varepsilon\zeta E$ increases monotonically with κa from zero as $\kappa a = 0$ to unity as $\kappa a \rightarrow \infty$. For constant values of r/a and κa, this normalized fluid velocity is a monotonically increasing but not a very sensitive function of the magnitude of $Ze\zeta/kT$.

In Figure 3, the normalized electroosmotic velocity $-\eta u^{(e)}(b)/\varepsilon\zeta E$ of a symmetric electrolyte solution at the

$Ze\zeta/kT$. For fixed values of κa and $Ze\zeta/kT$, the fluid velocity is a monotonically decreasing function of φ [$=(a/b)^2$], as expected. The effect of the porosity $(1 - \varphi)$ of the fiber matrix on this velocity can be significant, even as the porosity is fairly high. Available experimental data on the electrophoretic mobility in suspensions of spherical[38,45−47] and rodlike[48,49] particles in general indicate a decrease of the particle mobility with an increase in the particle volume fraction. Our predictions in Figure 3a are consistent with these experimental results.

The normalized average electroosmotic velocity $-\eta\langle u^{(e)}\rangle/\varepsilon\zeta E$ ($=-\eta L_{12}/\varepsilon\zeta$) of a symmetric electrolyte solution in a fiber matrix in the axial direction, calculated using eq 18, is plotted versus $Ze\zeta/kT$ in Figure 4 for various values of φ and κa. This
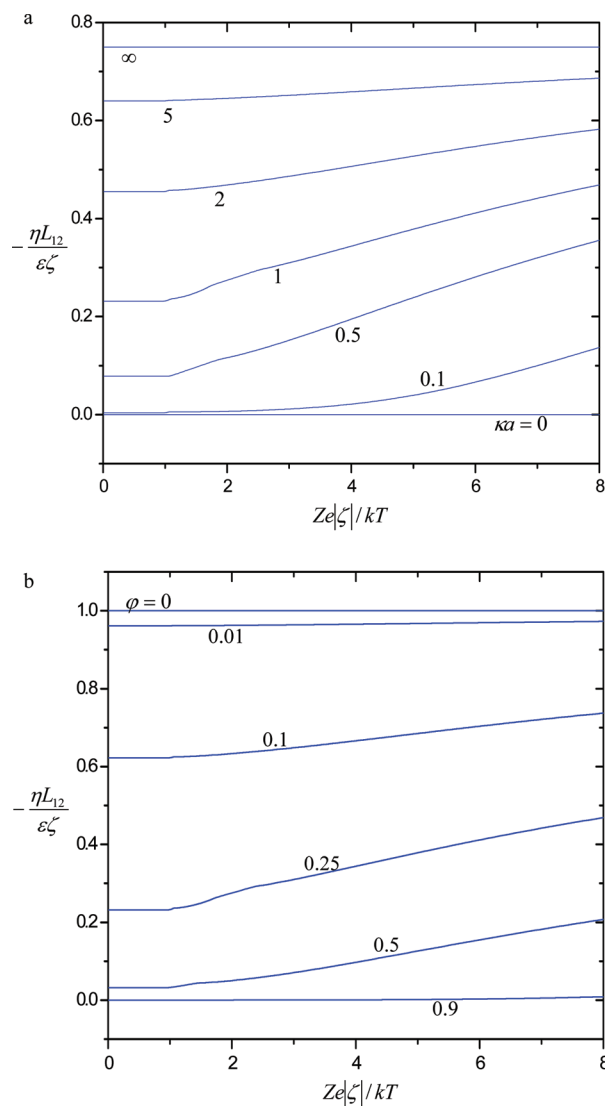

Figure 3. Plots of the normalized electroosmotic velocity $-\eta u^{(e)}(b)/\varepsilon\zeta E$ of a symmetric electrolyte solution at the outer boundary of a unit cell in the axial direction versus the electrokinetic radius κa: (a) $Ze|\zeta|/kT = 4$ and (b) $\varphi = 0.25$.

outer boundary of a unit cell, calculated using the available solution for $\psi(r)$,[43] is plotted against the electrokinetic radius κa for various values of the parameters $Ze\zeta/kT$ and φ. The calculations are presented up to $\varphi = 0.9$, which corresponds to the maximum attainable volume fraction (or minimum porosity) for a swarm of identical, parallel, circular cylinders (triangularly ordered).[44] Again, $-\eta u^{(e)}(b)/\varepsilon\zeta E$ increases monotonically with an increase in κa or $Ze\zeta/kT$ for a given value of φ. This normalized fluid velocity equals unity as $\kappa a \rightarrow \infty$ and vanishes as $\kappa a = 0$, regardless of the values of φ and

Figure 4. Plots of the normalized average electroosmotic velocity $-\eta L_{12}/\varepsilon\zeta$ of a symmetric electrolyte solution in a fiber matrix in the axial direction versus the dimensionless zeta potential $Ze\zeta/kT$: (a) $\varphi = 0.25$ and (b) $\kappa a = 1$.

fluid velocity is identical to that predicted by eq 19 for the case of $Ze|\zeta|/kT \leq 1$. Again, $-\eta\langle u^{(e)}\rangle/\varepsilon\zeta E$ increases monotonically with an increase in κa, an increase in $Ze|\zeta|/kT$, and a decrease in φ. In general, the effect of the parameter φ on this (superficial) electroosmotic velocity can be significant, but the influence of the parameter $Ze\zeta/kT$ on the normalized fluid velocity is

relatively weak. As expected, in the limiting case of $\kappa a \rightarrow \infty$, this fluid velocity equals $1 - \varphi$, irrespective of the values of φ and $Ze\zeta/kT$. In the limit $\varphi = 0$, $-\eta \langle u^{(e)} \rangle / \varepsilon \zeta E = 1$ for any given values of κa and $Ze\zeta/kT$.

4. EFFECTIVE ELECTRIC CONDUCTIVITY AND STREAMING POTENTIAL

4.1. General Analysis. The electric current density $i(r)$ accompanying the electrokinetic flow of the electrolyte solution in the axial direction of the fibrous medium is

$$i = u(r)\,\rho_e(r) + \Lambda(r)E \tag{20}$$

Here, ρ_e is given by eq 2, u is given by eq 14, and Λ is the local electric conductivity of the solution, which can be written as

$$\Lambda = \sum_m z_m^2 e^2 n_m^\infty \frac{D_m}{kT} \exp\left(-\frac{z_m e \psi}{kT}\right) \tag{21}$$

where D_m is the diffusion coefficient of the ionic species m. The first term on the right-hand side of eq 20 is the contribution due to transport of electrolyte ions by the convection of the fluid, whereas the second term corresponds to the contribution of charges moving relative to the fluid via electrolytic conduction.

The average current density $\langle i \rangle$ over the cross section of a unit cell can be expressed in terms of the Onsager transport coefficients L_{21} and L_{22}:

$$\langle i \rangle = L_{21}P + L_{22}E \tag{22}$$

Note that $L_{21} = L_{12}$, as can be shown and is expected from the Onsager reciprocity principle,[12,50] and its result has been given by eq 18 or 19 and illustrated in Figure 4. In eq 22, L_{22} is also the effective electric conductivity in the axial direction of the fibrous medium:

$$L_{22} = \langle \Lambda \rangle + \frac{\varepsilon^2 \kappa^2}{\eta} \frac{2\varphi}{(\kappa a)^2} \int_a^b \left(\frac{d\psi}{dr}\right)^2 r\, dr \tag{23}$$

For a given electrolyte solution with known ionic diffusion coefficients, the integrations in eq 23 can be performed using the available solution for the electrostatic potential distribution $\psi(r)$ to yield L_{22} as a function of the parameters $z_m e \zeta/kT$, κa, and φ.

The streaming potential in the fibrous medium due to an applied pressure gradient P is an induced electric field, which is just sufficient to avoid net electric current. Letting $\langle i \rangle = 0$ in eq 22, one obtains the streaming potential (gradient) as $E = -PL_{21}/L_{22}$. Substitution of this streaming potential into eq 15 yields the superficial fluid velocity under the imposed pressure gradient. Clearly, the streaming potential exerts an electric body force on the ionic fluid and causes an electroosmotic countercurrent of the fluid to reduce the pressure-induced flow. This flow reduction could account for an increase in the apparent viscosity of the fluid in the fibrous medium relative to the bulk value, known as the electroviscous retardation effect.

4.2. Case of Low Electric Potential. If eq 8 for $\psi(r)$ with the Debye−Hückel approximation is used, eq 23 for the effective electric conductivity in the axial direction of the fibrous medium can be analytically calculated to yield

$$L_{22} = \Lambda^\infty\left[1 - \varphi - I\beta\frac{e\zeta}{kT} + \left(J_1\gamma\frac{\varepsilon k^2 T^2}{\eta e^2} + J_2\alpha\right)\left(\frac{e\zeta}{kT}\right)^2\right] \tag{24}$$

where

$$\alpha = \frac{\sum_m z_m^4 n_m^\infty D_m}{\sum_m z_m^2 n_m^\infty D_m} \tag{25}$$

$$\beta = \frac{\sum_m z_m^3 n_m^\infty D_m}{\sum_m z_m^2 n_m^\infty D_m} \tag{26}$$

$$\gamma = \frac{\sum_m z_m^2 n_m^\infty}{\sum_m z_m^2 n_m^\infty D_m} \tag{27}$$

$$I = \frac{2\varphi}{\kappa a}\frac{G_1(a)}{G_0(a)} \tag{28}$$

$$J_1 = \frac{2}{b^2}\int_a^b \frac{G_0(r)}{G_0(a)}\left[1 - \frac{G_0(r)}{G_0(a)}\right]r\, dr \tag{29}$$

$$J_2 = \frac{1}{b^2}\int_a^b \left[\frac{G_0(r)}{G_0(a)}\right]^2 r\, dr \tag{30}$$

and $\Lambda^\infty = \Lambda(\psi = 0) = \sum_m z_m^2 e^2 n_m^\infty D_m/kT$ and is the specific conductance of the bulk fluid with negligible surface conductance.

The coefficients I, J_1, and J_2 in eq 24 for the effective electric conductivity expanded in terms of ζ are functions of the parameters κa and φ only. In this equation, the term containing J_1 comes from the last term in eq 23 or the contribution due to the electroosmotic flow of the electrolyte solution in the fiber matrix, whereas all the other terms (containing $1 - \varphi$, I, and J_2 of zeroth order, first order, and second order, respectively, in $e\zeta/kT$) result from the substitution of eq 21 into $\langle \Lambda \rangle$, which is the average of the local electric conductivity of the solution over a cross section of the unit cell. Note that, for a general electrolyte solution, the complete $O(\zeta^2)$ term in eq 24 should also include the contribution of this order in $\psi(r)$, which was neglected in eq 8. For a symmetric electrolyte solution, however, eq 24 is exact to this order since the $O(\zeta^2)$ term in $\psi(r)$ disappears.
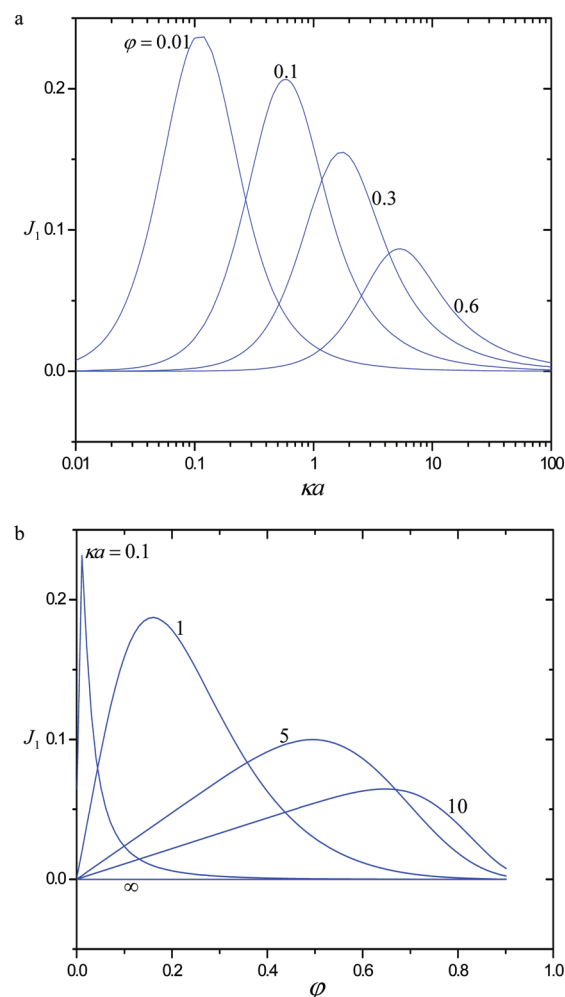
4.3. Results and Discussion. Figure 5 shows the plots of the dimensionless coefficient I of the $O(\zeta)$ term in eq 24 for the effective electric conductivity in a fiber matrix in the axial direction as a function of the parameters κa and φ. Similar to the effective conductivity in the direction normal to the fiber axes,[41] this coefficient is always a positive value, and thus, the presence of the surface charge of the cylinders increases this effective conductivity for any porosity of the fibrous medium if the product of β and ζ is negative and decreases it if this product is positive. Namely, the surface charge reduces the conductivity if the co-ions are more mobile than the counterions, and this phenomenon was also shown in the calculations for the conductivity of symmetric electrolytes within charged capillaries at low zeta potential values using a space charge model.[51] For a given value of φ, the coefficient I
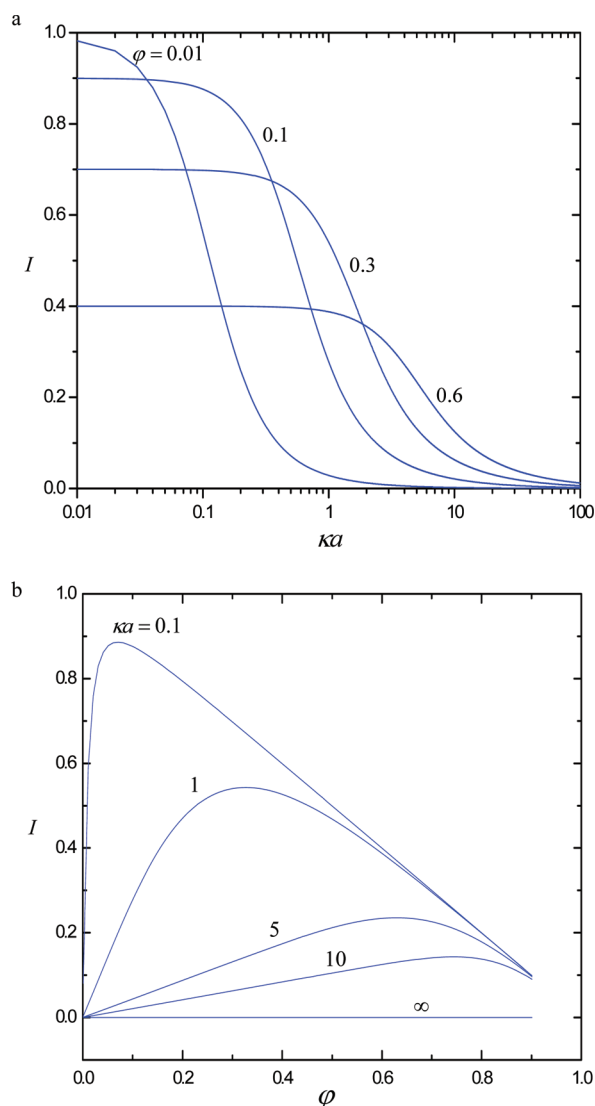
Figure 5. Plots of the dimensionless coefficient I in eq 24 for the effective conductivity in a fiber matrix in the axial direction versus the parameters κa and φ.
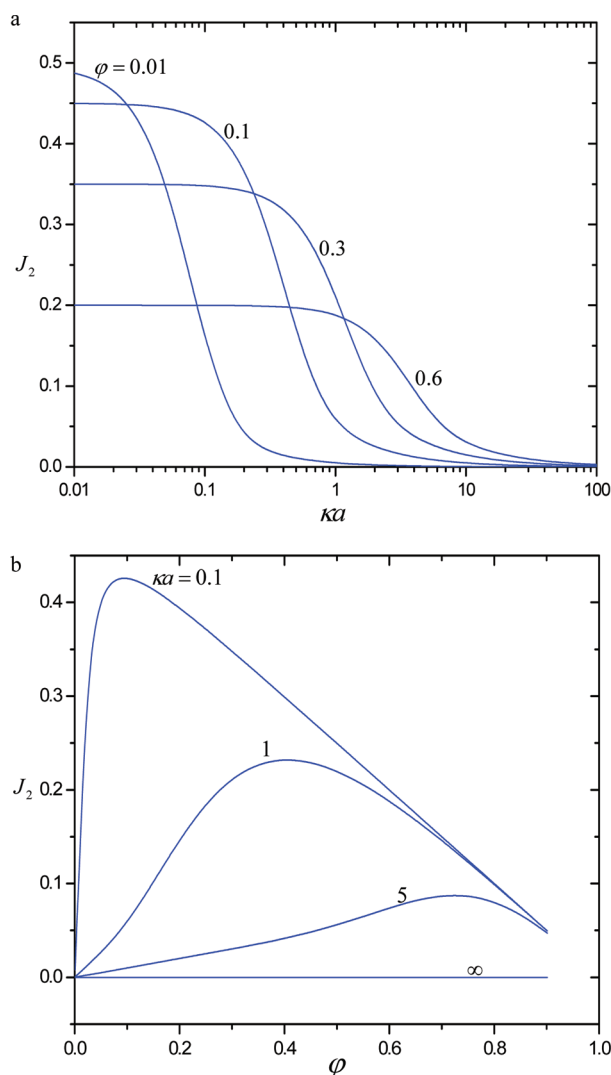

Figure 6. Plots of the dimensionless coefficient J_1 in eq 24 for the effective conductivity in a fiber matrix in the axial direction versus the parameters κa and φ.

or the effect of the surface charge on the effective conductivity decreases monotonically with an increase in κa and vanishes as $\kappa a \to \infty$, since $\psi = 0$ and $\Lambda = \Lambda^{\infty}$ in the entire fluid solution in this limit. For a specified value of κa, I is maximal at some finite value of φ. It is understood that the coefficient I vanishes as $\varphi = 0$ since $\Lambda = \Lambda^{\infty}$ everywhere in the immense bulk fluid for this case, is also small as φ becomes large since the volume fraction of the nonconducting cylinders is high for this case, and thus has a maximum at some value of φ in between. The location of the maximum in I shifts to greater φ as κa increases. In general, the effect of the parameter φ on the coefficient I is significant, and the value of I is greater in the axial direction than in the transverse direction of the fibrous system.

The dimensionless coefficient J_1 of the $O(\zeta^2)$ term in eq 24 due to the contribution from the electroosmotic flow of the electrolyte solution in the fibrous medium is plotted versus the parameters κa and φ in Figure 6. Similar to the trend of the coefficient I for a fixed value of κa, J_1 is not a monotonic function of φ with a maximum and the location of this maximum shifts to greater φ as κa increases. It is understood that the coefficient J_1 vanishes as $\varphi = 0$ since the space charge

density ρ_e is zero everywhere in the immense bulk fluid for this case, is also small as φ becomes large since the superficial electroosmotic velocity of the ionic fluid is small (as shown in Figure 4b) for this case, and thus has a maximum at some value of φ in between. For a constant value of φ, a maximum of the coefficient J_1 also appears at some finite value of κa. As φ increases, this maximum occurs at a larger κa. In the limit $\varphi = 0$, $\kappa a = 0$, or $\kappa a \to \infty$, J_1 vanishes since $d\psi/dr = 0$ in the bulk fluid solution for all these cases.
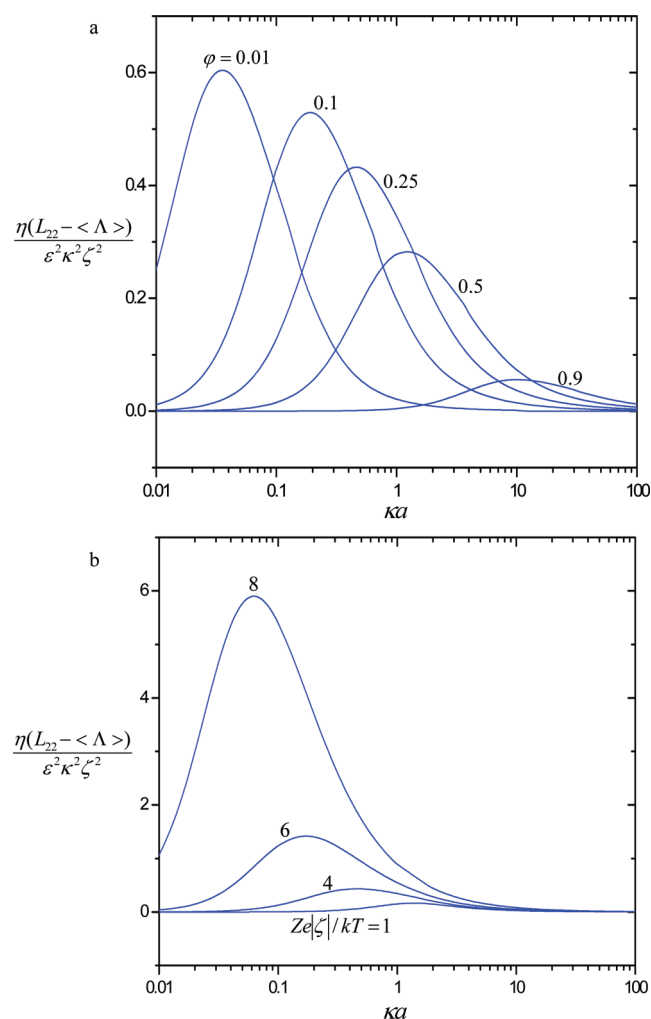
In Figure 7, the dimensionless coefficient J_2 of the $O(\zeta^2)$ term in eq 24 is plotted as a function of the parameters κa and φ. Both the coefficients J_1 and J_2 are always positive; thus, the $O(\zeta^2)$ contribution is to increase the effective electric conductivity of the fibrous medium. The trend of the dependence for the coefficient J_2 on κa and φ is analogous to that for I, but the value of J_2 is smaller by a factor of about 2.

The dimensionless electric conductivity coefficient $\eta(L_{22} - \langle\Lambda\rangle)/\varepsilon^2\kappa^2\zeta^2$ for the average current density due to the electroosmotic flow of the fluid solution of a symmetric electrolyte with the valence Z in a fiber matrix in the axial direction is plotted versus the electrokinetic radius κa in Figure 8 for various values of $Ze\zeta/kT$ and φ. Equation 23 incorporating with the solution for the electrostatic potential distribution $\psi(r)$ in the literature,[43] which is the same as eq 24 and $\eta(L_{22} - \langle\Lambda\rangle)/\varepsilon^2\kappa^2\zeta^2 = J_1\gamma\Lambda^{\infty}/\varepsilon\kappa^2$ for the case of low

Figure 7. Plots of the dimensionless coefficient J_2 in eq 24 for the effective conductivity in a fiber matrix in the axial direction versus the parameters κa and φ.

Figure 8. Plots of the normalized effective conductivity $\eta(L_{22} - \langle \Lambda \rangle)/\varepsilon^2\kappa^2\zeta^2$ due to the electroosmotic flow of a symmetric electrolyte solution in a fiber matrix in the axial direction versus the electrokinetic radius κa: (a) $Ze|\zeta|/kT = 4$ and (b) $\varphi = 0.25$.

electric potential ($Ze|\zeta|/kT \leq 1$), is used in these calculations. In general, the effect of interactions among the cylinders on the effective conductivity of the fibrous system is significant. Under an otherwise specified condition, the effective conductivity coefficient is not a monotonic function of the porosity $1 - \varphi$, analogous to the case of the coefficient J_1 illustrated in Figure 6 (and with the same physical explanation). This tendency is compatible with some recent experimental data[46] on the electric conductivity of a suspension of charged spherical particles at low volume fractions. For given values of $Ze\zeta/kT$ and φ, the current density contributed by the fluid flow is maximal at some finite values of κa (the location of this maximum shifts to smaller κa as the magnitude of $Ze\zeta/kT$ increases or φ decreases) and fades out when the value of κa is getting small or large. The reason for this behavior is obvious. In the limit $\kappa a = 0$, there exists no electroosmotic flow, as illustrated in Figures 2–4, whereas in the limit $\kappa a \to \infty$, the fluid is electrically neutral everywhere. For fixed values of κa and φ, the coefficient $\eta(L_{22} - \langle \Lambda \rangle)/\varepsilon^2\kappa^2\zeta^2$ increases monotonically with an increase in the magnitude of the parameter $Ze\zeta/kT$ and vanishes as this parameter equals zero.

In order for the reader to be able to relate our calculations with the measured value of electric conductivity in a fibrous medium, the demonstration of the behavior of the normalized total conductivity $\eta L_{22}/\varepsilon^2\kappa^2\zeta^2$ (including the average conductance $\langle \Lambda \rangle$ of the electrolyte solution at rest) is desirable. In Figure 9, we plot this total conductivity for the aqueous solution of 0.1 M potassium chloride (KCl, with the same value of the diffusion coefficients of the cation and anion) at room temperature, as an example, in a fiber matrix in the axial direction versus the parameter κa for various values of $e\zeta/kT$ and φ. Equations 21 and 23 with the available solution for $\psi(r)$ (ref 43) and the value $\varepsilon k^2 T^2/\eta D_{\pm} e^2 = 0.26$ (ref 52) are used in the calculations. A comparison between Figures 8 and 9 indicates that, for a given value of φ in this system, $\langle \Lambda \rangle$ contributes little to the normalized total conductivity when the value of κa is moderately small and the magnitude of $e\zeta/kT$ is large, but it becomes dominantly significant when the value of κa is relatively large or the magnitude of $e\zeta/kT$ is small. In the limits $\kappa a = 0$ and $\kappa a \to \infty$, the normalized total conductivities are finite constants, respectively, which come from the contribution of $\langle \Lambda \rangle$ entirely and, as expected, increase with a decrease in the magnitude of $e\zeta/kT$ ($\eta\langle \Lambda \rangle/\varepsilon^2\kappa^2\zeta^2$ is inversely proportional to ζ^2) or φ (the volume fraction of the electrolyte
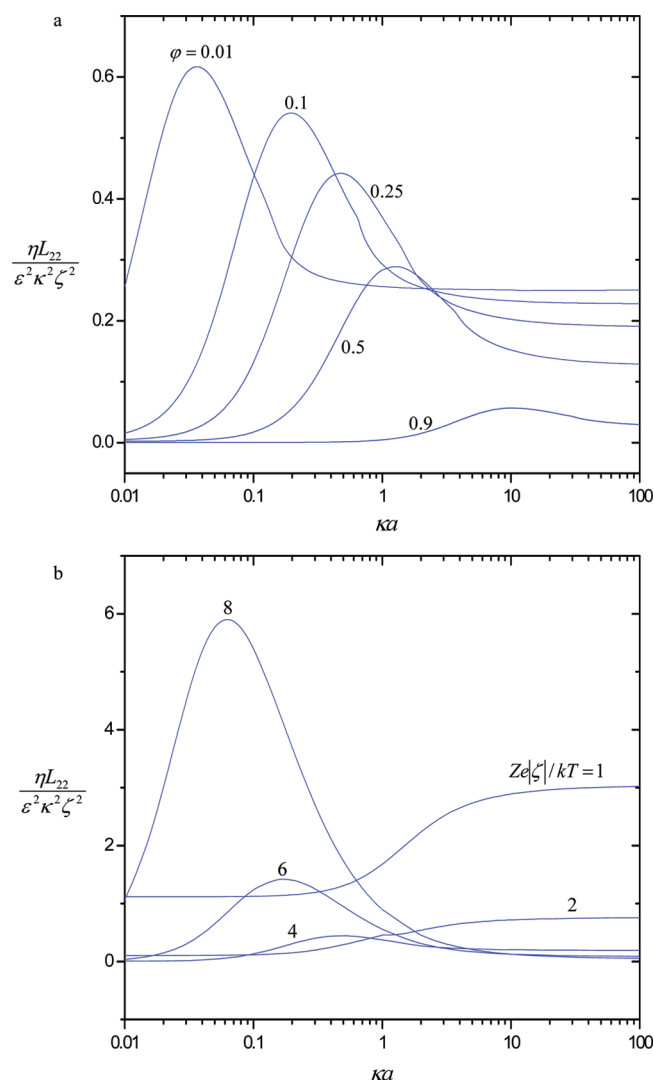
Figure 9. Plots of the normalized total effective conductivity $\eta L_{22}/\varepsilon^2\kappa^2\zeta^2$ of the aqueous solution of 0.1 M KCl at room temperature in a fiber matrix in the axial direction versus the electrokinetic radius κa: (a) $e|\zeta|/kT = 4$ and (b) $\varphi = 0.25$.

solution in the fibrous system is inversely proportional to φ). When the concentration of the electrolyte in the fluid solution is reduced (say, to 1 mM), the contribution of $\langle\Lambda\rangle$ to the total conductivity might become negligible except when the value of κa is extremely small or large or the magnitude of $e\zeta/kT$ approaches zero.

5. CONCLUSIONS

The steady electrokinetic flow of electrolyte solutions in an ordered array of identical, parallel, circular cylinders with arbitrary values of κa, $e\zeta/kT$, and φ is analyzed using the unit cell model in this paper. The cylinders may have a surface potential of arbitrary value. By solving the Poisson–Boltzmann equation and modified Navier–Stokes equation applicable to the system of a cylinder in a unit cell, the electrostatic potential distribution and the fluid velocity profile under an electric field and/or a pressure gradient imposed uniformly in the axial direction are obtained. Analytical expressions and numerical results for the electroosmotic velocity and effective electric conductivity in the fibrous medium as functions of relevant parameters are also presented. The effect of the porosity (1 −

φ) of the fiber matrix is interesting and can be significant under appropriate conditions. Although experimental results on the electroosmotic velocity and effective conductivity are available in the literature for suspensions of charged spheres,[37,38,45−47,53] the relevant experimental data for fibrous systems would be needed to confirm the validity of our cell-model results at various ranges of κa, $e\zeta/kT$, and φ.

The electroosmosis and electric conduction in a fibrous medium constructed by a homogeneous array of identical, parallel, charged, circular cylinders filled with an electrolyte solution in the direction normal to the axes of the cylinders were investigated by using a similar unit cell model with the assumption that the system is only slightly distorted from equilibrium, and analytical results of the electroosmotic velocity and effective electric conductivity as functions of relevant parameters were obtained for the case of low surface potential.[41] For the general problem of electroosmosis and electric conduction of ionic fluids in the fibrous medium caused by an applied electric field in an arbitrary direction with respect to the axes of the cylinders, which is linear in its governing equations and boundary conditions for the case of low surface potential and slightly distorted double layers from equilibrium, the solution of the electroosmotic velocity and effective electric conductivity can be obtained by the vectorial addition of the previous result for the transverse electrokinetic flow and the present result for the axial transport. Thus, the dependence of the electroosmotic velocity and effective conductivity on the respective angle between the applied electric field and the fiber axes can be examined using these results.

■ AUTHOR INFORMATION

Corresponding Author

*Telephone: 886-2-33663048. Fax: +886-2-2362-3040. E-mail: huan@ntu.edu.tw.

Notes

The authors declare no competing financial interest.

■ REFERENCES

(1) Henry, D. C. *Proc. R. Soc. London, Ser. A* **1931**, *133*, 106.
(2) Booth, F. *Proc. R. Soc. London, Ser. A* **1950**, *203*, 514.
(3) Booth, F. *J. Chem. Phys.* **1954**, *22*, 1956.
(4) O'Brien, R. W.; White, L. R. *J. Chem. Soc., Faraday Trans. 2* **1978**, *74*, 1607.
(5) O'Brien, R. W. *J. Colloid Interface Sci.* **1983**, *92*, 204.
(6) Ohshima, H.; Healy, T. W.; White, L. R. *J. Chem. Soc., Faraday Trans. 2* **1983**, *79*, 1613.
(7) Ohshima, H.; Healy, T. W.; White, L. R.; O'Brien, R. W. *J. Chem. Soc., Faraday Trans. 2* **1984**, *80*, 1299.
(8) Keh, H. J.; Liu, Y. C. *J. Colloid Interface Sci.* **1997**, *195*, 169.
(9) Ding, J. M.; Keh, H. J. *Langmuir* **2003**, *19*, 7226.
(10) Huang, Y. C.; Keh, H. J. *Langmuir* **2005**, *21*, 11659.
(11) Burgreen, D.; Nakache, F. R. *J. Phys. Chem.* **1964**, *68*, 1084.
(12) Rice, C. L.; Whitehead, R. *J. Phys. Chem.* **1965**, *69*, 4017.
(13) Keh, H. J.; Liu, Y. C. *J. Colloid Interface Sci.* **1995**, *172*, 222.
(14) Szymczyk, A.; Aoubiza, B.; Fievet, P.; Pagetti, J. *J. Colloid Interface Sci.* **1999**, *216*, 285.
(15) Keh, H. J.; Tseng, H. C. *J. Colloid Interface Sci.* **2001**, *242*, 450.
(16) Berli, C. L. A.; Olivares, M. L. *J. Colloid Interface Sci.* **2008**, *320*, 582.

(17) Jamaati, J.; Niazmand, H.; Renksizbulut, M. *Int. J. Therm. Sci.* **2010**, *49*, 1165.

(18) Levine, S.; Neale, G. H. *J. Colloid Interface Sci.* **1974**, *47*, 520.

(19) Zharkikh, N. I.; Borkovskaya, Yu. B. *Colloid J. USSR (Engl. Transl.)* **1982**, *43*, 520.

(20) Kozak, M. W.; Davis, E. J. *J. Colloid Interface Sci.* **1986**, *112*, 403.

(21) Ohshima, H. *J. Colloid Interface Sci.* **1999**, *210*, 397.

(22) Johnson, T. J.; Davis, E. J. *J. Colloid Interface Sci.* **1999**, *215*, 397.

(23) Ding, J. M.; Keh, H. J. *J. Colloid Interface Sci.* **2001**, *236*, 180.

(24) Carrique, F.; Cuquejo, J.; Arroyo, F. J.; Jimenez, M. L.; Delgado, A. V. *Adv. Colloid Interface Sci.* **2005**, *118*, 43.

(25) Keh, H. J.; Liu, C. P. *J. Phys. Chem. C* **2010**, *114*, 22044.

(26) Ohshima, H. *J. Colloid Interface Sci.* **1999**, *212*, 443.

(27) Hsu, W. T.; Keh, H. J. *Colloid Polym. Sci.* **2004**, *282*, 985.

(28) Cuquejo, J.; Jimenez, M. L.; Delgado, A. V.; Arroyo, F. J.; Carrique, F. *J. Phys. Chem. B* **2006**, *110*, 6179.

(29) Keh, H. J.; Wei, Y. K. *Langmuir* **2002**, *18*, 10475.

(30) Wei, Y. K.; Keh, H. J. *J. Colloid Interface Sci.* **2002**, *248*, 76.

(31) Lou, J.; Lee, E. *J. Phys. Chem. C* **2008**, *112*, 12455.

(32) Happel, J. *AIChE J.* **1958**, *4*, 197.

(33) Kuwabara, S. *J. Phys. Soc. Jpn.* **1959**, *14*, 527.

(34) Dukhin, A. S.; Shilov, V.; Borkovskaya, Yu. *Langmuir* **1999**, *15*, 3452.

(35) Zholkovskij, E. K.; Czarnecki, J.; Masliyah, J. H. *J. Colloid Interface Sci.* **2001**, *234*, 293.

(36) Happel, J. *AIChE J.* **1959**, *5*, 174.

(37) Watillon, A.; Stone-Masui, J. *J. Electroanal. Chem.* **1972**, *37*, 143.

(38) Zukoski, C. F.; Saville, D. A. *J. Colloid Interface Sci.* **1987**, *115*, 422.

(39) O'Brien, R. W. *J. Colloid Interface Sci.* **1981**, *81*, 234.

(40) Anderson, J. L. *Ann. N.Y. Acad. Sci.* **1986**, *469* (Biochem.Eng. 4), 166.

(41) Keh, H. J.; Wu, Y. Y. *J. Phys. Chem. B* **2011**, *115*, 9168.

(42) Philip, J. R.; Wooding, R. A. *J. Chem. Phys.* **1970**, *52*, 953.

(43) Keh, H. J.; Hsu, L. Y. *Microfluid. Nanofluid.* **2009**, *7*, 773.

(44) Berryman, J. G. *Phys. Rev. A* **1983**, *27*, 1053.

(45) Palberg, T.; Medebach, M.; Garbow, N.; Evers, M.; Fontecha, A. B.; Reiber, H.; Bartsch, E. *J. Phys.: Condens. Matter* **2004**, *16*, S4039.

(46) Medebach, M.; Jordan, R. C.; Reiber, H.; Schope, H.-J.; Biehl, R.; Evers, M.; Hessinger, D.; Olah, J.; Palberg, T.; Schonberder, E.; Wette, P. *J. Chem. Phys.* **2005**, *123*, 104903.

(47) Lobaskin, V.; Dunweg, B.; Medebach, M.; Palberg, T.; Holm, C. *Phys. Rev. Lett.* **2007**, *98*, 176105.

(48) Deggelmann, M.; Graf, C.; Hagenbuchle, M.; Hoss, U.; Johner, C.; Kramer, H.; Martin, C.; Weber, R. *J. Phys. Chem.* **1994**, *98*, 364.

(49) Hoss, U.; Batzill, S.; Deggelmann, M.; Graf, C.; Hagenbuchle, M.; Johner, C.; Kramer, H.; Martin, C.; Overbeck, E.; Weber, R. *Macromolecules* **1994**, *27*, 3429.

(50) Hunter, R. J. *Zeta Potential in Colloid Science*; Academic Press: London, 1981.

(51) Szymczyk, A.; Fievet, P.; Aoubiza, B. *Desalination* **2002**, *151*, 177.

(52) van de Ven, T. G. M. *Colloidal Hydrodynamics*; Academic Press: London, 1989.

(53) Bellini, T.; Degiorgio, V.; Mantegazza, F.; Marsan, F. A.; Scarnecchia, C. *J. Chem. Phys.* **1995**, *103*, 8228.